Inorganic Chemistry

Article

pubs.acs.org/IC

Organometallic Ni Pincer Complexes for the Electrocatalytic Production of Hydrogen

Oana R. Luca,[†] James D. Blakemore,[†] Steven J. Konezny,[†] Jeremy M. Praetorius,[†] Timothy J. Schmeier,[†] Glendon B. Hunsinger,*[,‡] Victor S. Batista,*[,†] Gary W. Brudvig,*[,†] Nilay Hazari,*[,†] and Robert H. Crabtree*[,†]

[†]Department of Chemistry, Yale University, 225 Prospect Street, New Haven, Connecticut 06520-8107, United States

[‡]Department of Geology and Geophysics, Earth Systems Center for Stable Isotopic Studies, Yale University, 210 Whitney Avenue, New Haven, Connecticut 06511, United States

Supporting Information

ABSTRACT: Nonplatinum metals are needed to perform cost-effective water reduction electrocatalysis to enable technological implementation of a proposed hydrogen economy. We describe electrocatalytic proton reduction and H_2 production by two organometallic nickel complexes with tridentate pincer ligands. The kinetics of H_2 production from voltammetry is consistent with an overall third order rate law: the reaction is second order in acid and first order in catalyst. Hydrogen production with 90−95% Faradaic yields was confirmed by gas analysis, and UV−vis spectroscopy suggests that the ligand remains bound to the catalyst over the course of the reaction. A computational study provides mechanistic insights into the proposed catalytic cycle. Furthermore, two proposed intermediates in the proton reduction cycle were isolated in a representative system and show a catalytic response akin to the parent compound.

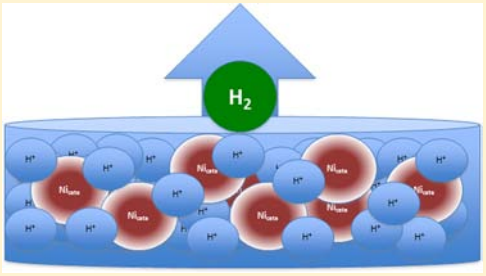

INTRODUCTION

Sustainable production of hydrogen is currently sought in the context of alternative energy strategies,[1,2] and low-cost proton reduction catalysts are of interest.[3,4] The hydrogenase enzymes have served as inspiration for a large number of model compounds[5−7] and H^+ reduction catalysts. Catalysts that model hydrogenases have now achieved essentially reversible H_2/H^+ equilibrium[8] using bimetallic [Fe−Fe] and [Fe−Ni] active sites.

Large-scale commercial use of Pt, the most active proton reduction catalyst, is prohibitively costly.[9] Among nonprecious metals, catalysis by complexes of Co,[10] Mo,[11,12] Ni[13−16] has been reported. Various factors affect the efficacy of these catalysts, including the solubility, stability, solvent, and choice of proton source. For example, DuBois and co-workers note an improvement of up to 60% in turnover number (TON) on addition of water to a nonaqueous system in which organic acids are employed,[14] while Jacques et al.[15] report drastic variations in turnover frequencies (TOFs) in macroscopic measurements of hydrogen production in a series of Co and Ni diimine dioxime catalysts in the presence of different proton donors with varying pK_a's.

A large body of work involving hydrogenase mimics, specifically Ni tetraphosphine complexes with pendant basic sites, has come from DuBois and co-workers.[17] These complexes not only act as electrocatalysts for proton reduction, but are also shown to catalyze the reverse process, hydrogen oxidation. The amine basic sites in the catalyst structure are thought to aid in stabilizing a bound hydrogen molecule, facilitate H_2 cleavage, and mediate proton shuttling to and from the Ni metal center. The best system gave a TOF of 106,000 s^{-1} in acetonitrile, in the presence of 1.2 M water which is an order of magnitude higher than the turnovers reported for hydrogenase enzymes, however operating at a much higher overpotential of ∼600 mV.[18] When a closely related catalyst to DuBois' system was tethered to a carbon nanotube, a turnover rate of 20,000 h^{-1}, or ∼333 s^{-1} was obtained from a 1 h electrolysis. After 10 h, the TON was 35,000, or ∼58 s^{-1}.[19] Light-driven hydrogen production was also seen in aqueous conditions with a similar system.[20]

In organometallic chemistry, pincer ligands are used to support catalysts for a variety of different reactions, owing to the high stability they impart to transition metal complexes[21] and the tunability of their steric and electronic properties. In previous work, we reported a tridentate coordination compound performing proton electroreduction in aqueous conditions.[22] Here, we report organometallic Ni complexes having pincer ligands that act as efficient electrocatalysts for proton reduction.

RESULTS AND DISCUSSION

Pincer Catalysis. Pincer compounds **1** and **2** depicted in Figure 1, although known,[23,24] have not previously been investigated in the context of proton reduction electrocatalysis.

Received: January 2, 2012
Published: July 31, 2012

   dx.doi.org/10.1021/ic300009a | *Inorg. Chem.* 2012, 51, 8704−8709

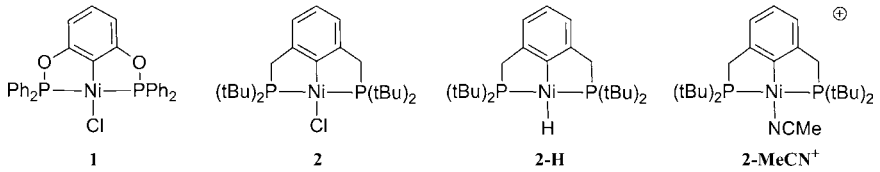

Figure 1. Nickel complexes used in the study of proton-reduction electrocatalysis.[23,24]

Their electrochemistry has now been studied in a standard 0.1 M acetonitrile/supporting electrolyte solution to determine their reduction potentials and establish any correlation between their catalytic activity and the ligand donor power (Figure 2).

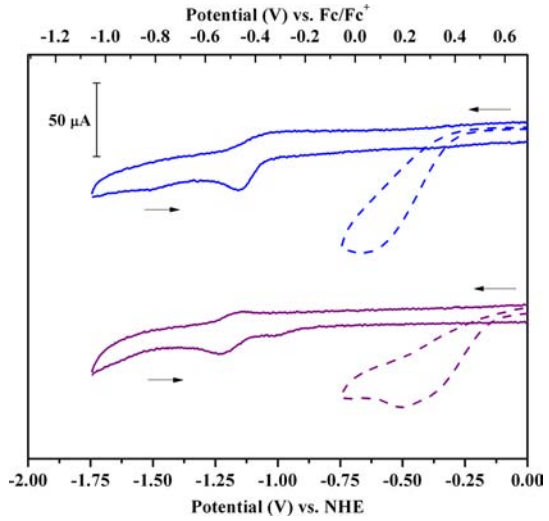

Figure 2. Solid lines: Nonaqueous electrochemistry of compounds **1** and **2**: 2 mM Ni complex in a 0.1 M NBu_4BF_4 acetonitrile solution at a glassy carbon electrode (100 mV/s) *top to bottom*: *blue* **1**; *purple* **2**. See Supporting Information for CVs of complexes **1** and **2** at different scan rates. Dashed lines: 2 mM solutions of complexes **1** and **2** in a 0.1 M NBu_4BF_4 acetonitrile solution with 20 μL 1 M HCl at 100 mV/s.

Our results confirm the expectation that a more strongly donor ligand framework stabilizes the higher oxidation state and makes metal reduction more difficult (See Figure 2 and Supporting Information for details).

Complexes **1** and **2** show similar electrochemical behavior. They both show a single reduction wave which we assign to a Ni^{II}/Ni^{I} couple. Complex **1** is more easily reduced than complex **2** which is consistent with the more donating framework of the PCP ligand in complex **2**.[25]

Incremental addition of aliquots of a 1 M HCl solution to complexes **1** and **2** led to a progressive increase in the current observed by voltammetry in this nickel pincer series (see Supporting Information). Figure 2 shows comparative cyclic voltammograms (CVs) of the pincer complexes in the presence of 20 μL of 1 M HCl. Compound **1** showed an irreversible wave with a less negative onset potential than the one observed for **2** under the same conditions. As expected, increasingly donor ligands appear to provide more negative onset potentials. Both waves are consistent with catalytic H_2 production, although the onset of catalysis is at much higher potentials than the reduction potentials of **1** and **2** in the absence of acid, an explanation for which is presented later. Plots of current density vs applied potential were constructed for catalysts **1** and **2** (Table 1 and Supporting Information, S2) and show a more negative overpotential at 1.5 mA cm^{-2} for **2** (−0.370 V), than for **1** (−0.345 V).

Table 1. Relative Rates of Proton Reduction in a 0.1 M NBu_4BF_4 Acetonitrile Solution and Overpotentials of Catalysts 1 and 2 at 1.5 mA cm^{-2}

catalyst	k (M^{-2} s^{-1})	TOF (s^{-1})	rate (M s^{-1})[a]	overpotential[b] at 1.5 mA cm^{-2}	faradaic yield[c]
1	$0.55 \times 10^4 \pm 0.32 \times 10^3$	54.6	0.275	−0.370 V	90% ± 3%
2	$2.9 \times 10^4 \pm 1.7 \times 10^3$	209	1.045	−0.345 V	95% ± 4%

[a]Calculated for 0.1 M H^+, 5 mM catalyst, using the method described by DuBois et al.[26] [b]Value determined from plots of current density vs applied potential constructed from chronoamperograms (dwell time: 60 s) at progressively more negative potentials corrected for $[H^+]$ = 0.037 M (the pH = −log$[H^+]$ = 1.42, $E^{o\prime}$ = −59 mV/pH*1.42 = −84 mV vs NHE). The working electrode was a 3 mm diameter glassy carbon disk. Measurements were performed with magnetic stirring, using 5.2 mL acetonitrile solutions containing 200 μL of 1 M aqueous HCl at catalyst concentrations of 0.2 mM with Ar purge. [c]From bulk electrolyses at −0.6 V vs NHE, (details in the Experimental Section and Supporting Information).

The rates of H_2 production were measured from voltammetry in acetonitrile (Table 1) using the method of DuBois and co-workers[14] described in detail in the Supporting Information. Our data are consistent with an overall third order rate law: the reaction is second order in acid and first order in catalyst. Catalyst **2** has a TOF of 209 s^{-1} under the reaction conditions, which is faster than catalyst **1** (54.6 s^{-1}). The Faradaic yield of H_2 production by **1** and **2**, measured using bulk electrolysis followed by quantitative mass spectrometry detection of H_2, is excellent, with approximately 90% yield observed in both cases. We believe that our catalysts are operationally homogeneous as UV−vis spectra of the catholyte before and after electrolyses show that the characteristic spectroscopic features of the catalysts are maintained, suggesting that significant decomposition is not occurring. Furthermore, when the electrode was removed after electrolyses, rinsed, and immersed in fresh electrolyte, no catalytic response was observed. This suggests an insoluble heterogeneous nickel catalyst is not being deposited on the electrode. The difference in catalytic rates based on the ligand is also consistent with a homogeneous system. Overall, our complexes appear to be slower catalysts in acetonitrile than DuBois' Ni tetraphosphine systems,[14,17,18] but they operate at similar overpotentials. However, direct comparison is complicated because of differences in the exact experimental conditions.

Proposed Catalytic Cycle and Mechanistic Experiments. Although the mechanism for proton reduction using tetraphosphine systems such as those described by DuBois is relatively well understood,[17] we were interested in comparing it to our PCP supported systems. As in previous studies, we

dx.doi.org/10.1021/ic300009a | Inorg. Chem. 2012, 51, 8704−8709

applied density functional theory (DFT) with the B3LYP functional to characterize the structural and spin/electronic properties of the reaction intermediates and perform free energy calculations.[22,27] Our calculated cycle for proton reduction catalyzed by **2** can be observed in Scheme 1, with

Scheme 1. Proposed Catalytic Cycle of Proton Reduction Supported by DFT Calculations at the B3LYP/LANL2DZ/cc-pVTZ Level of Theory Using [2-MeCN]$^+$ Formed after Loss of Cl$^-$ in MeCN

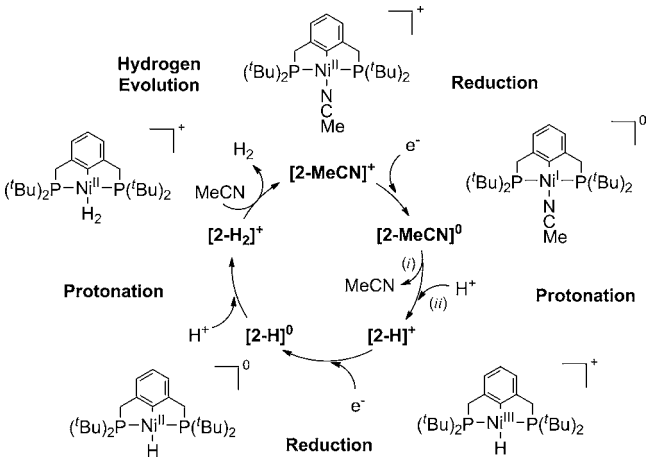

Table 2. Comparison of Relative Free Energies in Solution ΔG(MeCN) from DFT Calculations of Intermediates in Proton Reduction Using 2

compound	ΔG(MeCN) (kcal mol^{-1})	ΔG(MeCN) vs NHE[a] (eV)
[**2-MeCN**]$^+$	0	0
[**2-MeCN**]^0	−64.8	1.57
[**2-H**]$^+$	−72.0	1.26
[**2-H**]^0	−177.6	1.16
[**2-H$_2$**]$^+$	−192.7	0.51
[**2-MeCN**]$^+$ + H$_2$ − 2H$^+$ − 2e$^-$	−204.4	0

[a]Assumes a normal hydrogen electrode potential of 4.48 V in MeCN.

energies of the intermediates provided in Table 2. We believe that (PCP)NiCl (**2**) serves as a precatalyst and the active species is the solvento complex [**2-MeCN**]$^+$. Subsequently, one electron reduction of [**2-MeCN**]$^+$ generates the Ni^I species [**2-MeCN**]^0 (Scheme 1), which is consistent with our assignment of the first reduction in the CV of **2** to the Ni^{II}/Ni^I couple. Sequential MeCN ligand loss (−4.8 kcal mol^{-1}) followed by protonation (−2.3 kcal mol^{-1}) of [**2-MeCN**]^0 to form the Ni^{III} hydride [**2-H**]$^+$ is downhill in energy, thus indicating a favorable process. The calculated pK_a of [**2-H**]$^+$ is 1.7, similar to the pK_a of 1.8 measured for [Ni(cyclam)(H)]$^{2+}$ (cyclam = 1,4,8,1 L-tetraazacyclotetradecane) in aqueous solution.[28] The fact that these Ni hydrides with N-based ligands are less acidic than Ni hydrides with P-based ligands[29] is consistent with pK_a trends observed in other metal hydrides.[30] Analysis of the spin density on [**2-H**]$^+$ confirms that it is a Ni^{III} species with no significant delocalization of the spin onto the ligand framework. This stands in contrast to our recent report of a Ni proton reduction catalyst supported by an NNN pincer ligand, which undergoes an initial ligand centered reduction.[22] It indicates that a redox active ligand is not required for pincer complexes to be active for proton reduction. To complete the cycle, the Ni^{III} intermediate [**2-H**]$^+$ is further reduced by one electron to give the square planar Ni^{II} hydride [**2-H**]^0 which then undergoes protonation to give the dihydrogen complex [**2-H$_2$**]$^+$, followed by loss of H$_2$ to regenerate [**2-MeCN**]$^+$. The third order rate law experimentally determined for catalysts **1** and **2** suggests that the turnover limiting step in our catalytic cycles involve protonation of the Ni−H intermediate [**2-H**]^0 to [**2-H**]$^+$. Although we cannot exclude the limiting step being loss of H$_2$, relative energies indicate that this should be a spontaneous process for **2**.

Our mechanism for H$_2$ production is analogous to DuBois' system;[17] however, the PCP framework that supports the catalytically active compound **2** provides a tractable representative system for the isolation of possible intermediates. For the purposes of probing this hypothesis, we independently prepared [**2-MeCN**]$^+$ via chloride abstraction from (PCP)NiCl (**2**). The hydride complex **2-H** was also synthetically accessible by literature methods.[24]

The redox behavior of complex **2-H** shown in Figure 3 was followed by cyclic voltammetry using 0.1 M NBu$_4$BF$_4$ and 2

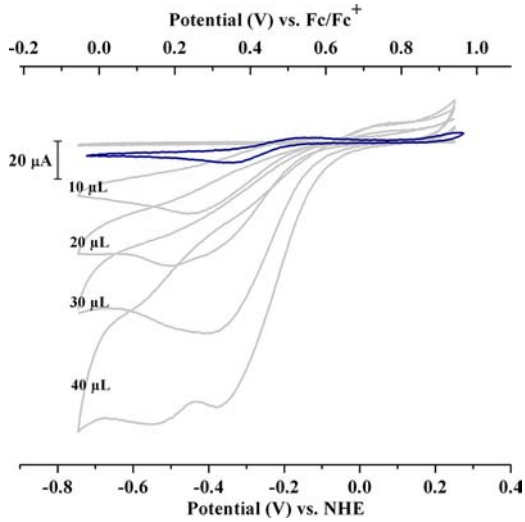

Figure 3. *Blue:* CV of 2 mM **2-H** in a 0.1 M NBu$_4$BF$_4$ acetonitrile solution under air/water free conditions 100 mV/s. *Gray:* CVs of parent compound **2** (top gray CV completely silent in the scanned region) involved in proton reduction with 4 × 10 μL increments of 1 M HCl.

mM catalyst precursor solution in a Schlenk cell under rigorously anhydrous conditions. The change from the halide in **2** to the much softer H$^-$ ligation in **2-H** causes a dramatic shift of the Ni^{II}/Ni^I couple by almost 1 V in the positive direction to −0.2 V vs NHE. This wave also coincides with the onset of proton reduction catalysis in the parent halide **2**, as seen in Figure 2. This observation is consistent with **2-H** being a key intermediate in the overall catalytic reaction. Upon incremental addition of 10 μL of HCl to **2-H** (see Supporting Information), bubbles are immediately observed followed by a steadily increasing current response analogous to the chloride compound under the same conditions. We, therefore, assign the observed electrochemistry to the [**2-H**]$^+$/[**2-H**]^0 step (Scheme 1) and its participation in the catalytic cycle.

dx.doi.org/10.1021/ic300009a | *Inorg. Chem.* 2012, 51, 8704−8709

The protonation of **2-H** with 1 equiv of HBF_4 in acetonitrile results in the clean formation of the solvento cation $[\mathbf{2\text{-}MeCN}]^+$ (eq 1). This was confirmed by comparison of the ^1H

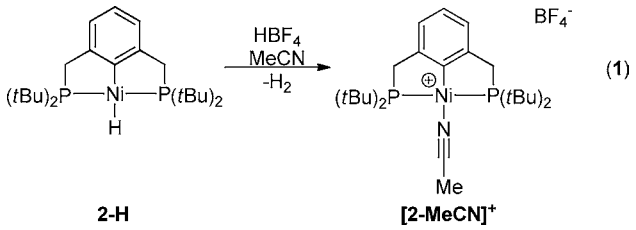

(1)

NMR spectrum with an authentic sample of $[\mathbf{2\text{-}MeCN}]^+$ prepared through the abstraction of Cl^- from **2**. When **2-H** was protonated in a J. Young NMR tube, H_2 was detected by ^1H NMR spectroscopy. This is consistent with our proposed mechanism involving protonation of the hydride, to generate a short-lived dihydrogen complex $[\mathbf{2\text{-}H_2}]^+$ in Scheme 1, followed by coordination of solvent to close the cycle. A molecular hydrogen complex is a probable intermediate in the conversion of **2-H** to $[\mathbf{2\text{-}MeCN}]^+$ but is presumably too unstable to observe spectroscopically in acetonitrile in the time scale of the experiment.

In the absence of protons, $[\mathbf{2\text{-}MeCN}]^+$ shows an irreversible Ni^{II}/Ni^{I} wave at a potential intermediate between those of **2** and **2-H** (Supporting Information, Figure S1−3) which we believe corresponds to the $[\mathbf{2\text{-}MeCN}]^+/[\mathbf{2\text{-}MeCN}]^0$ in the catalytic cycle depicted in Scheme 1. The irreversibility and magnitude of the wave is caused by the inability of the acetonitrile ligand to stabilize the Ni^I center being formed (See Supporting Information for CVs at different scan rates). The reduction of the cationic $[\mathbf{2\text{-}MeCN}]^+$ may also be coupled to a chemical process at the electrode surface. It has previously been observed that changes in ligation at the metal center alter the observed electrochemical behavior.[31]

In acidic conditions, $[\mathbf{2\text{-}MeCN}]^+$ shows an increasing cathodic current response akin to **2-H** and **2** (Supporting Information, Figure S1−3). The onset of the catalytic wave is in the same region as the Ni^{II}/Ni^{I} wave exhibited by **2-H**, supporting our hypothesis that the solvento complex is involved in the catalytic cycle. In general, the onset of a catalytic process is often associated with a distinct reversible wave corresponding to a redox change at a metal center. In the present case, we believe that the observed electrocatalytic response is a result of reduction of an in situ generated pincer-Ni-H species in the presence of protons. To confirm our hypothesis, we observe that the onset of proton reduction electrocatalysis for **2**, **2-H**, and $[\mathbf{2\text{-}MeCN}]^+$ occurs at the same potential (Figure 4 and Supporting Information, Figure S1−3) under similar conditions.

CONCLUSIONS

Two organometallic Ni^{II} pincer complexes are active catalysts for electrochemical proton reduction. Bulk electrolysis experiments followed by macroscopic determination of the quantity of H_2 produced demonstrated good Faradaic yields (90%−95%). Two of the possible intermediate species were isolated and shown to be catalytically active using the PCP ligand framework. Computation provides corroboration for the proposed catalytic cycle. Further tuning of the ligand will be explored to look for even more active catalysts that operate at lower overpotentials.

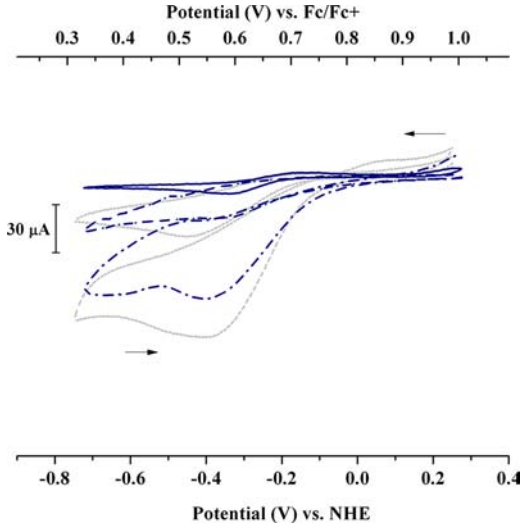

Figure 4. Overlay of CVs of acetonitrile (0.1 M NBu_4BF_4) solutions 2 mM **2** with 10 (*solid gray*) and 20 μL of 0.1 M aqueous HCl (*dotted gray*), **2-H** (*solid navy*), **2-H** with 10 μL of 1 M aqueous HCl (*dash-dot navy*), and **2-H** with 20 μL of 1 M aqueous HCl (*dash-dot navy*).

EXPERIMENTAL SECTION

General Methods. All reagents were received from commercial sources and used without further purification unless otherwise specified. Solvents were dried by passage through a column of activated alumina followed by storage under dinitrogen. NMR spectra were recorded at room temperature on Bruker AMX-400 or 500 MHz spectrometers unless otherwise specified. Chemical shifts are reported with respect to residual internal protio solvent for ^1H and $^{13}C\{^1H\}$ NMR spectra and to an external standard for $^{31}P\{^1H\}$ spectra (85% H_3PO_4 at 0.0 ppm). Literature procedures were utilized to synthesize compounds **1**, **2**, and **2-H**.[23−25]

Electrochemical Experiments, Bulk Electrolyses, and Gas Analysis. CVs in acetonitrile were collected on glassy carbon electrodes (3 mm diameter from Bioanalytical Systems) with a platinum wire counter electrode and a silver wire reference electrode in a BASI Double Junction Reference Electrode Setup MF-2030 (referenced to NHE with ferrocene as external standard $E_{1/2}$ = 690 mV vs NHE). An alternate ferrocene reference scale is provided for all CVs. Measurements were performed in 0.1 M NBu_4BF_4 solutions at 2 mM concentration of the respective complexes. CVs were recorded after additions of 4 × 10 μL of 1 M HCl via volumetric syringe (10 μL of 1 M HCl corresponds to $[H^+]$ = 10 mM, 20 μL $[H^+]$ = 20 mM, 30 μL $[H^+]$ = 30 mM and 40 μL corresponds to $[H^+]$ = 40 mM, respectively). CV measurements of **2-H** were performed under Argon in a custom-built air sensitive voltammetry cell equipped with a septum injection port. All other CVs were recorded after rigorous exclusion of air via Argon purge. Data workup was performed on OriginPro v8.0988 and AfterMath Data Organizer Version 1.2.3383.

Plots of current density vs applied potential were constructured from chronoamperometry experiments (dwell time: 60 s) at potentials lower than 0 V (vs NHE) at a glassy carbon electrode in a single-chamber, three-electrode configuration. The experiments were performed in 5.2 mL of 0.1 M NBu_4BF_4 acetonitrile solutions containing 0.2 mM catalyst and 200 μL of a 1 M aqueous HCl solution. Vigorous magnetic stirring was used to avoid diffusion limitations from concentration gradients at the working electrode.

The order of reaction with respect to acid was determined by analysis of CVs of 2 mM catalyst solutions with different acid concentrations. To a 0.1 M NBu_4BF_4 acetonitrile solution containing 2 mM catalyst (from the CVs of which i_p was determined at different scan rates), 5 μL increments were added of an aqueous 1 M HCl solution also containing 0.1 M NBu_4BF_4. The voltammograms thus collected at each acid concentration for several scan rates were used to obtain catalytic currents, denoted i_c. The ratio of i_c/i_p was plotted

dx.doi.org/10.1021/ic300009a | Inorg. Chem. 2012, 51, 8704−8709

against acid concentration for the different scan rates. From the approximately linear behavior at each scan rate, we conclude that our system obeys a rate law which is second order in acid. The slopes of the scan rate-dependent data were then used to calculate the third order rate constants. Graphs and description of the methods are available in the Supporting Information.

The order in catalyst was determined from voltammograms collected at 100 mV/s with 3.5 mL of a 0.1 M NBu_4BF_4 acetonitrile solution with a concentration of 2.82 mM catalyst and 4 mM acid. Increments of 0.5 mL of a 0.1 M NBu_4BF_4 acetonitrile solution were added, and the dilutions were adjusted to maintain a constant acid concentration. We assumed no significant variations in the acid concentration throughout the experiment. From each voltammogram, i_c was plotted against catalyst concentration. From the linearity of the resulting graph, we conclude that at reasonably low catalyst concentration first order behavior is observed. Graphs and description of the methods are available in the Supporting Information.

Controlled potential headspace H_2 detection experiments were performed in a custom built two cylinder 50 mL bulk electrolysis H cell anode/cathode chamber separated by a coarse frit. The working electrode was a reticulated vitreous carbon electrode from Bioanalytical Systems MF-2077 referenced vs Ag/AgCl in KCl_{sat}. Headspace H_2 detection was performed at the Yale Department of Geology on a calibrated mass spectrometer: dual inlet Thermo Finnegan MDT 253 and an airtight bulk electrolysis H Cell equipped with a sampling port. One milliliter volumes of gas were compressed in the bellow and then opened to the mass spectrometer.

Computational Methods. Density functional calculations were carried out using Gaussian 09.[32] Gas phase free energy changes were calculated at the B3LYP/LANL2DZ/cc-pVTZ level, using minimum energy structures obtained at the B3LYP/LANL2DZ level of theory. Full optimization of geometry was performed without any symmetry constraint, followed by analytical computation of the Hessian matrix to identify the nature of the located extrema as minima. The solvation free energies ΔG_{solv} for species other than solvated H^+ were computed using the Polarizable Continuum Model as implemented in Gaussian 09 based on the gas-phase geometries with dielectric constant of ε = 35.7 for MeCN. The cc-pVTZ basis set was used for all atoms except Ni for which the LANL2DZ basis set was substituted. Free energies in solution were determined using the gas-phase free energies, the solvation free energies, and the Born−Haber thermodynamic cycle.[22,27] For the solvated proton, a free energy in MeCN of −266.48 kcal mol^{-1} was used based on an experimentally determined[33] solvation free energy of $\Delta G^{H+}{}_{solv}$(MeCN) = −260.20 kcal mol^{-1}.

Synthesis and Characterization of New Compounds and Experimental Procedure. *Synthesis of [(PCP)Ni(NCCH$_3$)]$^+$[BF$_4$]$^-$ [2-MeCN]$^+$.* To (PCP)NiCl (**2**) (40 mg, 82 μmol) and $AgBF_4$ (16 mg, 82 μmol) was added 1 mL of acetonitrile at 25 °C. The reaction was stirred overnight and then filtered through Celite. The solvent was removed in vacuo to give [(PCP)Ni(NCCH$_3$)]$^+$[BF$_4$]$^-$ [**2-MeCN**]$^+$ as a yellow-orange powder (47 mg, 99% Yield). Single crystals suitable for X-ray crystallography were grown from saturated acetonitrile solutions containing [**2-MeCN**]$^+$ (see Supporting Information, S7). HR FT-ICR MS: Found (calcd for $C_{26}H_{46}NNiP_2$): m/z = $(M)^+$ 492.2467 (492.2459), $(M\text{-}NCCH_3)^+$ 451.2193 (451.2196). ^{1}H NMR ($NCCD_3$, 500.0 MHz): δ 6.94−6.98 (3H, m, Ar*H*), 3.32 (4H, t, PCH_2Ar, J = 4.2 Hz), 1.37 (36H, t, $PC(CH_3)_3$, J = 6.6 Hz). $^{13}C\{^1H\}$ NMR ($NCCD_3$, 125.8 MHz): δ 154.6 (t, J = 11.4 Hz), 153.0 (t, J = 13.9 Hz), 135.9 (s), 128.0 (*s*), 123.4 (t, J = 9.1 Hz), 35.9 (t, J = 7.6 Hz), 33.4 (t, J = 13.7 Hz), 29.7 (s). $^{31}P\text{-}\{^1H\}$ NMR ($NCCD_3$, 161.9 MHz): 80.1 ppm.

Protonation of [(PCP)NiH] (2-H). To [(PCP)NiH] (**2-H**) (3 mg, 6.2 μmol) dissolved in 0.5 mL of d_3-acetonitrile in a J. Young NMR tube was added 1 equiv of HBF_4 in 10 μL of H_2O at 25 °C. Mixing of the two solutions occurred only after the NMR cap was replaced. ^{1}H NMR spectroscopy displayed a characteristic resonance for H_2 along with peaks corresponding to [(PCP)Ni(NCCH$_3$)]$^+$[BF$_4$]$^-$ [**2-MeCN**]$^+$.

■ ASSOCIATED CONTENT

Ⓢ Supporting Information

Additional CVs, further experimental details, details of the crystal structure determination of [**2-MeCN**]$^+$ and *xyz* coordinates and energies of optimized structures. This material is available free of charge via the Internet at http://pubs.acs.org.

■ AUTHOR INFORMATION

Corresponding Author

*Fax: (+)1 203 432 6144. E-mail: glendon.hunsinger@yale.edu (G.B.H.), victor.batista@yale.edu (V.S.B.), gary.brudvig@yale.edu (G.W.B.), nilay.hazari@yale.edu (N.H.), robert.crabtree@yale.edu (R.H.C.).

Notes

The authors declare no competing financial interest.

■ ACKNOWLEDGMENTS

The work was supported as part of the Center for Electrocatalysis, Transport Phenomena, and Materials (CETM) for Innovative Energy Storage, an Energy Frontier Research Center funded by the U.S. Department of Energy, Office of Basic Energy Sciences, under Award Number DE-SC00001055 (R.H.C. and V.S.B.). We also gratefully acknowledge the Argonne-Northwestern Solar Energy Research (ANSER) Center, EFRC under Award Number DE-PS02-08ER15944 for support of the electrochemical studies (G.W.B., R.H.C., and J.D.B.). V.S.B. acknowledges supercomputer time from NERSC, XSEDE, and the High-Performance Computing facilities at Yale University. We also thank Daryl Smith for help with the electrochemical cell design and Professor Mark Johnson, Arron Wolk, and Dr. Rachael Relph for characterization of [**2-MeCN**]$^+$ by mass spectroscopy.

■ REFERENCES

(1) Artero, V.; Fontecave, M. *Coord. Chem. Rev.* **2005**, *249*, 1518−1535.

(2) Vincent, K. A.; Parkin, A.; Armstrong, F. A. *Chem. Rev.* **2007**, *107*, 4366−4413.

(3) Crabtree, R. H. *Energy Production and Storage: Inorganic Chemical Strategies for a Warming World*; Wiley-VCH: Chichester, U.K., 2010; pp 3−19.

(4) Rosi, N. L.; Eckert, J.; Eddaoudi, M.; Vodak, D. T.; Kim, J.; O'Keeffe, M.; Yaghi, O. M. *Science* **2003**, *300*, 1127−1130.

(5) Barton, B. E.; Whaley, M. C.; Rauchfuss, T. B.; Gray, D. L. *J. Am. Chem. Soc.* **2009**, *131*, 6942−6943. Madden, C.; Vaughn, M. D.; Díz-Pérez, I.; Brown, K. A.; King, P. W.; Gust, D.; Moore, A. L.; Moore, T. A. *J. Am. Chem. Soc.* **2012**, *134*, 1577−1582.

(6) Gloaguen, F.; Lawrence, J. D.; Rauchfuss, T. B.; Bénard, M.; Rohmer, M. *Inorg. Chem.* **2002**, *41*, 6573−6582.

(7) (a) Gloaguen, F.; Rauchfuss, T. B. *Chem. Soc. Rev.* **2009**, *38*, 100−108. (b) Losse, S.; Vos, J. G.; Rau, S. *Coord. Chem. Rev.* **2010**, *254*, 2492−2504.

(8) Rakowski-DuBois, M.; DuBois, D. L. *Acc. Chem. Res.* **2009**, *42*, 1974−1982.

(9) (a) Bockris, J. O'M.; Conway, B. E. *Trans. Faraday Soc.* **1949**, *45*, 989−999. (b) Ezaki, H.; Morinaga, M.; Watanabe, S. *Electrochim. Acta* **1993**, *38*, 557−564.

(10) Stoichiometric cobalt mediated H_2 production: (a) Connolly, P.; Espenson, J. H. *Inorg. Chem.* **1986**, *25*, 2684−2688. (b) Koelle, U.; Ohst, S. *Inorg. Chem.* **1986**, *25*, 2689−2694. (c) Chao, T.-H.; Espenson, J. H. *J. Am. Chem. Soc.* **1978**, *100*, 129−133. Cobalt electrocatalysis (d) Hu, X.; Brunschwig, B. S.; Peters, J. C. *J. Am. Chem. Soc.* **2007**, *129*, 8988−8998. (e) Kellett, R. M.; Spiro, T. G. *Inorg. Chem.* **1985**, *24*, 2373−2377. (f) Szymczak, N. K.; Berben, L. A.; Peters, J. C. *Chem. Commun.* **2009**, 6729−6731. (g) Berben, L. A.;

Peters, J. C. *Chem. Commun.* **2010**, 398−400. Supported electrocatalyst (h) Baffert, C.; Artero, V.; Fontecave, M. *Inorg. Chem.* **2007**, *46*, 1817−1824. (i) Bernhardt, P. V.; Jones, L. A. *Inorg. Chem.* **1999**, *38*, 5086−5090. (j) Pantani, O.; Naskar, S.; Guillot, R.; Millet, P.; Anxolabéhère-Mallart, E.; Aukauloo, A. *Angew. Chem., Int. Ed.* **2008**, *47*, 9948−9950. (k) Razavet, M.; Artero, V.; Fontecave, M. *Inorg. Chem.* **2005**, *44*, 4786−4795. (l) Fihri, A.; Artero, V.; Razavet, M.; Baffert, C.; Leibl, W.; Fontecave, M. *Angew. Chem., Int. Ed.* **2008**, *47*, 564−567. (m) Stubbert, B. D.; Peters, J. C.; Gray, H. B. *J. Am. Chem. Soc.* **2011**, *133*, 18070−18073. Cobalt photocatalysis (n) Dempsey, J. L.; Brunschwig, B. S.; Winkler, J. R.; Gray, H. B. *Acc. Chem. Res.* **2009**, *42*, 1995−2004. (o) McNamara, W. R.; Han, Z.; Alperin, P. J.; Brennessel, W. W.; Holland, P. L.; Eisenberg, R. *J. Am. Chem. Soc.* **2011**, *133*, 15368−15371. Studies of photogenerated intermediates: (p) Dempsey, J. L.; Winkler, J. R.; Gray, H. B. *J. Am. Chem. Soc.* **2010**, *132*, 16774−16776. (q) Dempsey, J. L.; Winkler, J. R.; Gray, H. B. *J. Am. Chem. Soc.* **2010**, *132*, 1060−1065. (r) Du, P.; Schneider, J.; Luo, G.; Brennessel, W. W.; Eisenberg, R. *Inorg. Chem.* **2009**, *48*, 4952−4962. (s) Du, P.; Knowles, K.; Eisenberg, R. *J. Am. Chem. Soc.* **2008**, *130*, 12576−12577. (t) Fihri, A.; Artero, V.; Pereira, A.; Fontecave, M. *Dalton Trans.* **2008**, *41*, 5567−5569. (u) Probst, B.; Kolano, C.; Hamm, P.; Alberto, R. *Inorg. Chem.* **2009**, *48*, 1836−1843. (v) Lakadamyali, F.; Erwin, E. *Chem. Commun.* **2011**, *47*, 1695−1697. (w) Szajna-Fuller, E.; Bakac, A. *Eur. J. Inorg. Chem.* **2010**, 2488−2494. (x) Pantani, O.; Anxolabéhère-Mallart, E.; Aukauloo, A.; Millet, P. *Electrochem. Commun.* **2007**, *9*, 54−58 , both Co and Ni glyoximes.

(11) $\{CpMo(\mu\text{-}S)\}_2S_2CH_2$ as electrocatalyst for H_2 production: Appel, A. M.; DuBois, D. L.; Rakowski-DuBois, M. *J. Am. Chem. Soc.* **2005**, *127*, 12717−12726.

(12) $[(Py_5Me_2)Mo(CF_3SO_3)]^+$: Karunadasa, H. I.; Chang, C. J.; Long, J. R. *Nature* **2010**, *464*, 1329−1333.

(13) (a) Macrocyclic Nickel compound: Efros, L. L.; Thorp, H. H.; Brudvig, G. W.; Crabtree, R. H. *Inorg. Chem.* **1992**, *31*, 1722−1724. (b) Electrochemistry of nickel tetrazamacrocycles: Bernhardt, P. V.; Lawrence, G. A.; Sangster, D. F. *Inorg. Chem.* **1988**, *27*, 4055−4059.

(14) (a) $[Ni(P^{Ph}_2N^{C6H4\times2})_2]^{2+}$ as electrocatalysts for H_2 production: Kilgore, U. J.; Roberts, J. A. S.; Pool, D. H.; Appel, A. M.; Stewart, M. P.; Rakowski-DuBois, M.; Dougherty, W. G.; Kassel, W. G.; Bullock, R. M.; DuBois, D. L. *J. Am. Chem. Soc.* **2011**, *133*, 5861−5872. (b) Similar complexes have also been shown to perform CO_2 electroreduction as well as H_2 production: Rakowski-DuBois, M.; DuBois, D. L. *Acc. Chem. Res.* **2009**, *42*, 1974−1982.

(15) Ni and Co cobaloximes: Jacques, P.-A.; Artero, V.; Pecaut, J.; Fontecave, M. *Proc. Natl. Acad. Sci.* **2009**, *106*, 20627−20632.

(16) Angamuthu, R.; Bouman, E. *Phys. Chem. Chem. Phys.* **2009**, *11*, 5578−5583.

(17) Proton relays in Ni electrocatalysis: (a) Yang, J. Y.; Bullock, R. M.; Shaw, W. J.; Twamley, B.; Fraze, K.; DuBois, D. L.; Simone, R.; Rousseau, R.; DuPuis, M.; Rakowski-DuBois, M. *J. Am. Chem. Soc.* **2009**, *131*, 5935−5945. (b) Yang, J. Y.; Shentan, C.; Kassel, W. S.; Bullock, R. M.; DuBois, D. L.; Simone, R.; Rousseau, R.; DuPuis, M.; Rakowski-DuBois, M. *Chem. Commun.* **2010**, 46. (c) Rakowski-DuBois, M.; DuBois, D. M. *Chem. Soc. Rev.* **2009**, *38*, 62−72. (d) DuBois, D. L.; Morris, B. R. *Eur. J. Inorg. Chem.* **2011**, 1017−1027. (e) Jain, A.; Lense, S.; Linehan, J. C.; Raugei, S.; Herman, C.; DuBois, D. L. *Inorg. Chem.* **2011**, *50*, 4073−4085. The Co analogue has been reported (f) Wiedner, E. S.; Yang, J. Y.; Dougherty, W. J.; Kassel, W.; Bullock, R. M.; Rakowski-DuBois, M.; DuBois, D. L. *Organometallics* **2010**, *29*, 5390−5401. Theoretical work has been performed in (g) Small, Y. A.; DuBois, D. L.; Fujita, E.; Muckerman, J. T. *Energy Environ. Sci.* **2011**, *4*, 3008−3020.

(18) (a) Helm, M. L.; Stewart, M. P.; Bullock, R. M.; Rakowski-DuBois, M.; DuBois, D. L. *Science* **2011**, *333*, 863−866. A TOF of 9000 s^{-1} is reported for hydrogenase enzymes in (b) Frey, M. *ChemBioChem* **2002**, *3*, 153−160.

(19) Le Goff, A.; Artero, V.; Jousselme, B.; Tran, P. D.; Guilet, N.; Métayé, R.; Fihri, A.; Palacin, S.; Fontecave, M. *Science* **2009**, *326*, 1384−1387.

(20) McLaughlin, M. P.; McCormick, T. M.; Eisenberg, R.; Holland, P. L. *Chem. Commun.* **2011**, *47*, 7989−7991.

(21) Morales-Morales, D.; Jensen, C. *The Chemistry of Pincer Compounds*; Elsevier: Amsterdam, The Netherlands, 2007.

(22) Luca, O. R.; Konezny, S. J.; Blakemore, J. D.; Colosi, D. M.; Saha, S.; Brudvig, G. W.; Batista, V. S.; Crabtree, R. H. *New J. Chem.* **2012**, *36*, 1149−1152.

(23) Gomez-Benitez, B.; Baldovino-Pantaleon, O.; Herrera-Alvarez, C.; Toscano, R. A.; Morales-Morales, D. *Tetrahedron Lett.* **2006**, *47*, 5059−5062.

(24) Boro, B. J.; Duesler, E. N.; Goldberg, K. I.; Kemp, R. A. *Inorg. Chem.* **2009**, *48*, 5081−5087.

(25) Zhu, K.; Achord, P. D.; Zhang, X.; Krogh-Jespersen, K.; Goldman, A. S. *J. Am. Chem. Soc.* **2004**, *126*, 13044−13053.

(26) (a) Pool, D. H.; DuBois, D. L. *J. Organomet. Chem.* **2009**, *694*, 2858−2865. (b) Wilson, A. D.; Newell, R. H.; McNevin, M. J.; Muckerman, J. T.; Rakowski-DuBois, M.; DuBois, D. L. *J. Am. Chem. Soc.* **2006**, *128*, 358−366.

(27) (a) Konezny, S. J.; Doherty, M. D.; Luca, O. R.; Soloveichik, G. L.; Crabtree, R. H.; Batista, V. S. *J. Phys. Chem. C* **2012**, *116*, 6349−6356. (b) Batista, V. S.; Crabtree, R. H.; Konezny, S. J.; Luca, O. R.; Praetorius, J. M. *New J. Chem.* **2012**, *36*, 1141−1144. (c) Luca, O. R.; Wang, T.; Konezny, S. J.; Batista, V. S.; Crabtree, R. H. *New J. Chem.* **2011**, *35*, 998−999.

(28) Kelly, C. A.; Mulazzani, Q. G.; Venturi, M.; Blinn, E. L.; Rodgers, M. A. J. *J. Am. Chem. Soc.* **1995**, *117*, 4911−4919.

(29) DuBois, M. R.; DuBois, D. L. *Chem. Soc. Rev.* **2009**, *38*, 62−72.

(30) Zhu, Y.; Fan, Y. B.; Burgess, K. *J. Am. Chem. Soc.* **2010**, *132*, 6249−6253.

(31) (a) Blakemore, J. D.; Schley, N. D.; Balcells, D.; Hull, J. F.; Olack, G. W.; Incarvito, C. D.; Eisenstein, O.; Brudvig, G. W.; Crabtree, R. H. *J. Am. Chem. Soc.* **2010**, *132*, 16017−16029. (b) Brewster, T. P.; Blakemore, J. D.; Schley, N. D.; Incarvito, C. D.; Hazari, N.; Brudvig, G. W.; Crabtree, R. H. *Organometallics* **2011**, *30*, 965−973.

(32) Frisch, M. J.; et al. *Gaussian 09*, Revision A.1; Gaussian, Inc.: Wallingford, CT, 2009. See the Supporting Information for the complete reference.

(33) Kelly, C. P.; Cramer, C. J.; Truhlar, D. G. *J. Phys. Chem. B* **2007**, *111*, 408−422.